Number dependency in the compensated Penning trap

R. S. Van Dyck, Jr., F. L. Moore, D. L. Farnham, and P. B. Schwinberg
Department of Physics, FM-15, University of Washington, Seattle, Washington 98195
(Received 10 July 1989)

Due to the increasing role that highly charged ions play in high-precision mass-ratio measurements within a compensated Penning trap, it is imperative that we investigate the dependency of the normal-mode frequencies on the total number of trapped charges. The experimental number dependency has been measured for four different ion species with various states of ionization. The absolute shift in both the observable cyclotron and magnetron frequencies is 0.018(3) Hz per equivalent electronic charge for a trap with characteristic dimension of 0.114 cm (in a 5-T field). The source of this systematic dependency has been traced to image charges induced on the surface of the trapping electrodes, whose electric field at the ion's position near trap center is approximately linear in the displacement of the trapped ions. A simple spherical model has been developed that is useful as a guide in minimizing this systematic effect.

I. INTRODUCTION

The *compensated* Penning trap[1] very closely approximates the ideal Penning trap and in the past several years such traps have demonstrated a remarkable ability to produce highly precise measurements of certain fundamental quantities such as the electron's g factor and the electron-positron g-factor comparison,[2] the electron-positron mass ratio,[3] the proton-electron mass ratio,[4] and now the proton's atomic mass.[5] In the future, the use of compensated Penning traps for precision measurements will increase dramatically as illustrated by proposals to measure the $\bar{p}/p$ mass ratio,[6] the masses of nuclei far from stability,[7] the ^{3}H-^{3}He mass difference,[8–10] the fine structure constant,[8] and high-Z Lamb shifts.[11] Because of the increasing role which this apparatus is having in the field of high-precision metrology, it is imperative that its limitations and potential be investigated for possible future precision at the subpart per billion (ppb) level. Along these lines, the interesting observation of beats in the cyclotron resonance[12] may further increase the device's potential precision and put greater pressure upon understanding its limitations.

To put this analysis into perspective, a brief description of the experimental apparatus is in order. However, for a more complete description, see earlier accounts.[13–15] Figure 1 shows a simple three-electrode Penning trap with two endcaps and a ring electrode (all hyperboloids of revolution about the z axis), placed into a liquid-helium environment at the center of a highly stable and uniform magnetic field, B_0 obtained from a persistent field superconducting solenoid. Ions are generated by use of a field-emission electrode placed in one endcap, oriented to produce an ionizing electron beam along the z axis of symmetry. A dc potential V_0 is applied to the ring electrode with respect to grounded endcaps to produce axial confinement and the magnetic field overcomes the associated radial (antitrapping) electrostatic force. Once confined, the ion's axial motion at ω_z is driven like a har-

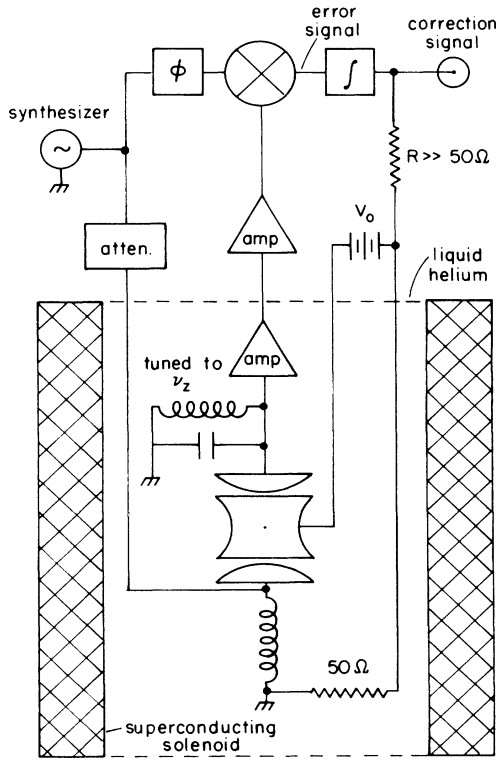

FIG. 1. Overall schematic of experiment. A three-electrode Penning trap is depicted at the center of a superconducting solenoid, and submerged in a liquid-helium environment. The grounded drive coil and signal-cap tuned circuit establish the axial trapping field by virtue of a ring electrode held at potential V_0. The feedback signal is generated by mixing the phase-shifted drive synthesizer with the amplified ion signal to produce an error signal. This error signal is integrated and fed back as a correction voltage to the ring bias circuitry, thereby producing a frequency lock.

monic oscillator using a very stable frequency synthesizer. The current induced in the signal endcap is observed as a voltage drop across a parallel LC circuit, tuned to the ion's axial frequency. This signal is amplified and mixed with the original (appropriately phase shifted) drive synthesizer to generate an error signal that can be integrated and fed back to the ring electrode. In this way, the ion's axial resonance is kept "frequency locked" to the drive oscillator. In the present ion work, the correction voltage is used as a frequency shift signal which represents the particle's noncentered position via the residual anharmonic terms in the basic trapping potential.

The compensated Penning trap itself is a five-electrode device that contains two additional "guard" electrodes placed between each endcap and the main ring electrode. These allow us to compensate for the fourth-order term in the trapping potential which is dominant by symmetry. In addition, the "quadring" Penning trap[13] contains an additional modification in which the ring electrode is split into four equal parts in order that the cyclotron motion may be efficiently driven and cooled as well as to allow for its direct detection. Figure 2 shows a cyclotron resonance for a single C^{4+} ion which is indirectly observed through the anharmonic shifts in the locked axial frequency. Traces are shown in both directions, each normally being preceded by strong axial sideband cooling[14] prior to excitation (though in general, very little energy is mixed into the magnetron, $\mathbf{E}\times\mathbf{B}$ drift motion). A weak rf drive field near the cyclotron's electric dipole resonance is swept through the resonant frequency and detection arises when the cyclotron orbit increases, producing a sharp signature in the correction voltage. Precision in this case is ± 3 parts in 10^{10}. However, the observation of beats, which can be clearly seen in Fig. 2 leading up to the sharp signature may offer us a means of obtaining an order of magnitude increase in precision.[12]

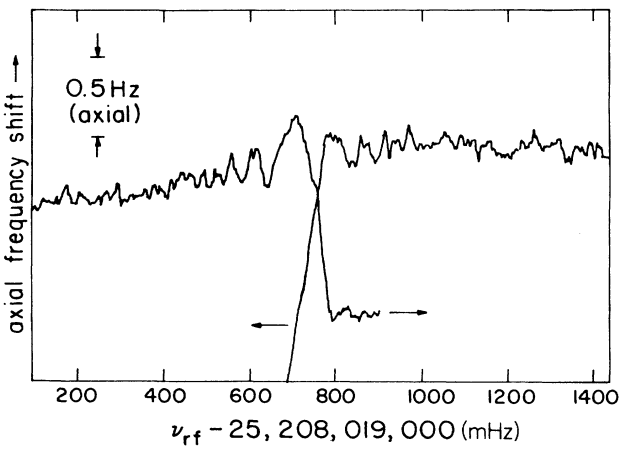

FIG. 2. Cyclotron resonance for a single C^{4+} ion. Upon absorbing the rf drive, the excitation is made observable in the correction signal through anharmonic terms in the trapping potential. Note the time-varying frequency of the beat note as the drive approaches resonance from above and below. Precision here approaches ± 0.3 ppb.

Therefore, the exact electrical environment of the trapped ion needs to be investigated to be sure that there are no systematic shifts which have not been taken into account. As our first step in this analysis, we investigate the effect that the trapped charge has on the electrostatic trapping potential.

In the following sections, the normal mode frequencies in a realistic Penning trap will be labeled according to the notation $\bar{\omega}$ (where $\bar{\omega}=2\pi\bar{\nu}$) to explicitly indicate that possible shifts exist whose source is not the standard quadratic trapping field. However, the conventional notation for the observed axial, magnetron, and cyclotron frequencies in an ideal Penning trap are ω_z, ω_m, and ω_c' (respectively) with the constraints that

$$\omega_m = \frac{\omega_z^2}{2\omega_c'} , \tag{1a}$$

$$\omega_c' = \omega_c - \omega_m , \tag{1b}$$

where

$$\omega_c = \frac{eB_0}{mc} \tag{1c}$$

is the trap-independent cyclotron frequency for a charge q with mass m located in a uniform magnetic field, B_0. This last frequency is taken as a measure of the ion's inertial mass. In Sec. II we present experimental evidence for the systematic dependency of the normal-mode frequencies upon the number of charges n isolated within the ideal Penning trap. In Sec. III we present the explanation for the systematic, based on a spherical model with image charge, and compare the results with what is observed. Finally, in Sec. IV we discuss the impact of this correction on precision mass measurements now and into the future.

II. EXPERIMENTAL OBSERVATIONS

This particular number-dependency effect does *not* depend on the anharmonic content of the potential distribution, but is intrinsic to the constraint of a charged particle surrounded entirely by conducting surfaces. Earlier, less well-compensated quadring Penning traps[16] have had larger number dependencies and sometimes with the opposite sign. These early traps displayed this larger effect primarily because of the intrinsic anharmonic nature of their potential wells. Present ion traps, however, are at least an order of magnitude more harmonic, and the explanation for the present effect must be found elsewhere.

The importance of the effect lies with the increasing use of multiply charged ions for precision spectroscopy. The size of the absolute shift will be shown to grow as the charge state increases. Initially, it was believed that a single ion would not show this number dependency since the most likely candidate was electrostatic space charge shifts. However, the model presented here indicates that even a single ion will have all of its normal mode frequencies shifted by the induced surface charge. The model therefore suggests that the proper approach is to extrapolate these frequencies to *zero* trapped ions, before determining the trap-independent cyclotron frequency, ω_c.

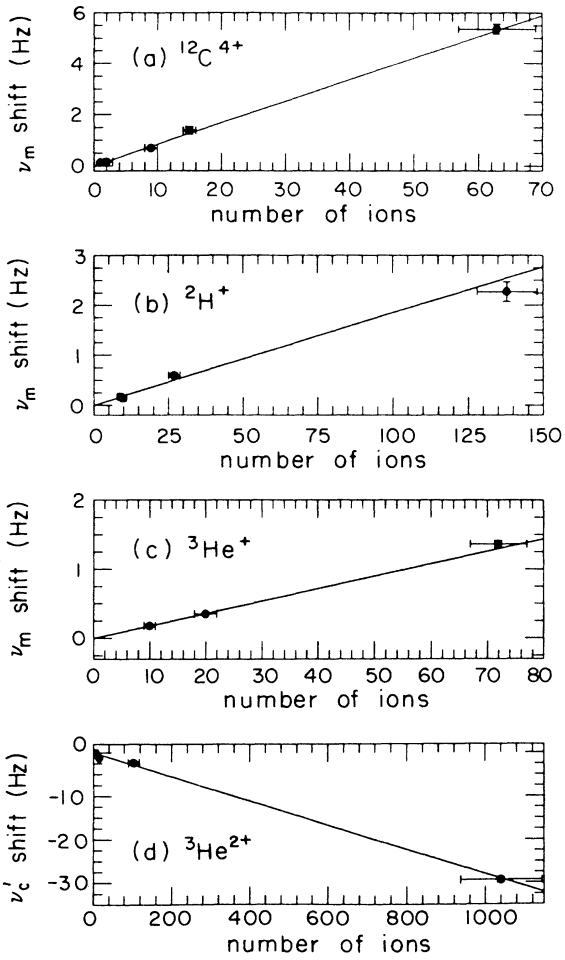

FIG. 3. Number dependency of various ions. The number of trapped ions is determined from the width of the axial resonance. In (a)–(c), the magnetron frequency shift is plotted vs the number of $^{12}C^{4+}$, $^{2}H^{+}$, and $^{3}He^{+}$ ions, respectively. In (d), the cyclotron frequency shift is plotted vs the number of $^{3}He^{2+}$. Also shown in each plot is a linear least-squares fit to the data.

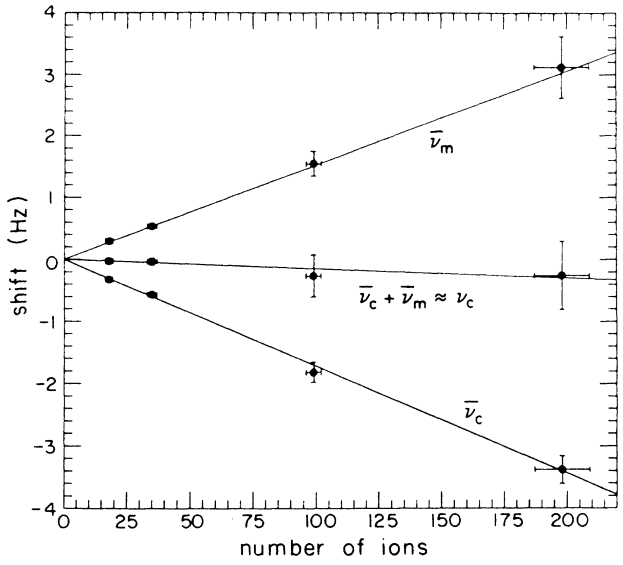

FIG. 4. Number dependency for protons. The shifts in the observed cyclotron frequency $\bar{\nu}_c$, the observed magnetron frequency $\bar{\nu}_m$, and the sum $\bar{\nu}_c+\bar{\nu}_m$ are plotted vs the number of ions. The sum is consistent with zero number dependency and is approximately equal to the trap-independent cyclotron frequency, ν_c.

Figures 3 and 4 show the measured number dependency for five examples of trapped ions ($^{12}C^{4+}$, $^{2}H^{+}$, $^{3}He^{+}$, $^{3}He^{2+}$, and $^{1}H^{+}$). The number n is obtained from the well-resolved axial resonance linewidth $\Delta\nu_z = n\delta\nu_1$, after a single ion linewidth has been resolved for at least one ion. Other single ion linewidths then scale as q_1^2/m_1 (and tuned circuit Q, etc.) where q_1 and m_1 are the reference ion's unit charge and mass, respectively. A well-resolved axial resonance will show some noise reduction due to the shorting out of the tuned circuit by the ion's effective series-equivalent lc representation.[17] Figures 3(a)–3(c) show the magnetron frequency shift plotted versus the number of ions and Fig. 3(d) is a similar plot for the cyclotron frequency shift. Figure 4 (for protons), however, shows the dependency for both the observed magnetron and cyclotron frequencies as well as their *sum* which is consistent with no number dependency. One can conclude from this that the number dependency manifests itself as a phase slippage (or frequency shift) only in the observed magnetron frequency and thus suggests an electrostatic origin. This follows from $\omega_c = \omega_c' + \omega_m$ which is obtained from the equation of motion for a charged particle in an ideal Penning trap and the fact that ω_c would not be constant for magnetic shifts. Table I summarizes the present data for the different ions with various masses and charge states. These results suggest that, for both the magnetron and cyclotron resonances, absolute shifts scale only with charge and the relative cyclotron shifts scale only with the ion's mass (assuming the trap constant and B_0 are held fixed). Thus, the average

TABLE I. Summary of number dependency for various ions. Values in parentheses denote the fitted uncertainty.

Ion	Mass (amu)	Charge (units of e)	Relative mass/charge	Abs. shift in (Hz/charge)	Rel. shift (ppb/ion)
$^{1}H^{+}$	1	1	1	0.0179(18)	0.23
$^{2}H^{+}$	2	1	2	0.0185(14)	0.48
$^{3}He^{+}$	3	1	3	0.0180(19)	0.72
$^{3}He^{2+}$	3	2	1.5	0.014(3)	0.55
$^{12}C^{4+}$	12	4	3	0.021(2)	3.33

shift in ν_m is 0.018(3) Hz/charge (for our present trap located in a 5 T magnetic field). This average reflects an overall uncertainty of 10% in the individual number calibration which is about twice the statistical uncertainty. Because of the linearity and obvious electrostatic nature of the shift, we conclude that image charges could be the source of the systematic effect.

III. SPHERICAL MODEL WITH IMAGE CHARGE

The effect that image charges have upon the normal modes of a trapped electron have been considered previously by Wineland and Dehmelt,[17] by Brown, Helmerson, and Tan,[18] and by Dehmelt.[19] In the treatment by Wineland and Dehmelt, the trap is replaced by a pair of grounded parallel plates, separated by the characteristic endcap-to-endcap distance. An infinite series of fictitious charges are placed along the z axis of symmetry (outside the parallel plate configuration) in order to meet the appropriate boundary conditions. The treatment by Brown *et al.* is much more rigorous whereby a longitudinal electric field is produced by the effective image charges in addition to a transverse component which they show is responsible for the microwave cavity modes seen by the cyclotron motion of an electron. The longitudinal component is the gradient of a radiation-gauge scaler potential whose major effect is to alter the electrostatic binding field generated by the standard quadrupole potential. Both of these treatments correctly conclude that the alteration in electrostatic binding can be safely ignored for the g-2 work;[2] however, as we show here, this is not the case for ions in our 3 times smaller trap with an order of magnitude more precisely measured cyclotron frequencies. It is also worth noting that in the treatment by Dehmelt,[19] the axial shift can be correctly obtained in the limit that $\omega=\omega_z$ for a spherical-wave model in which the cavity-reflected wave reacts back on the source of the dipole radiation at frequency ω inside a spherical cavity.

Since we wish only to get an estimate for the shifts to be expected for trapped ions as well as their general dependence on mass, charge, and geometry of the trap, we will consider the trap replaced by a grounded conducting spherical shell of radius a with the ion as a point charge located inside (see Fig. 5). A sphere is a reasonable approximation to the trap since the actual volume of space within which the charge moves is typically very small (less than 10^{-5} of the total trap volume) and located at the trap center. The charge $Q=nq_1$ located at position $\mathbf{r}$ relative to the center of the sphere induces an image charge Q' at some radius $\mathbf{r}'$ located *beyond* the inner conducting surface. The potential due to this image charge[20] will satisfy the boundary condition that $\Phi(a)=0$ only if

$$Q'=-\frac{aQ}{r} \quad \text{and} \quad \mathbf{r}'=\frac{a^2\mathbf{r}}{r^2} \ . \tag{2}$$

The corresponding electric field due to the point image charge at the *trapped ion's position* is according to Coulomb's law:

$$\mathbf{E}_{\text{image}}=\frac{-Q'\hat{\mathbf{r}}}{|\mathbf{r}'-\mathbf{r}|^2}=\frac{Qa\mathbf{r}}{(a^2-r^2)^2} \ . \tag{3}$$

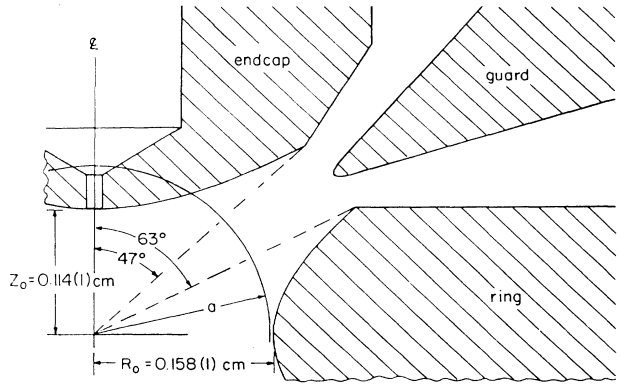

FIG. 5. Scale drawing of trap electrodes. The effective sphere radius $a\approx R_0$ is shown for comparison with the actual electrodes. Also, the break in endcap and ring electrodes (where contours deviate from hyperboloids) are at $\theta=47°$ and $\theta=63°$, respectively. The point of the guard electrode is at $\theta=56°$, but the exact guard contour is not critical in determining the effective image-charge sphere because of the $1/r^3$ dependence.

This image force can now be superimposed onto the usual electrostatic trapping fields (in terms of the same spherical coordinate, r)

$$\mathbf{E}_{\text{trap}}=-\nabla\left[\frac{V_0}{4d^2}(3z^2-r^2)\right] , \tag{4}$$

where V_0 is now the potential applied to the ring electrode with endcaps grounded, $2d^2=Z_0^2+\frac{1}{2}R_0^2$, and $2Z_0$ and $2R_0$ are minimum endcap separation and ring electrode diameter, respectively (see Fig. 5 for dimensions). By decomposition into cylindrical coordinates z,ρ and with $r\ll a$, we obtain the following total electric fields at the site of the trapped ion(s):

$$E_z=-\left[\frac{V_0}{d^2}-\frac{Q}{a^3}\right]z, \quad E_\rho=\left[\frac{V_0}{2d^2}+\frac{Q}{a^3}\right]\rho \ . \tag{5}$$

The axial equation of motion, $m_1\ddot{z}=q_1E_z$ for a particle of mass m_1 and charge q_1 (or equivalently, the center of mass) yields the shifted axial frequency $\bar{\omega}_{z,n}$ given by

$$\bar{\omega}_{z,n}^2=\frac{q_1V_n}{m_1d^2}-\Delta_n \tag{6}$$

with $\Delta_n\equiv nq_1^2/m_1a^3$ for n ions with charge q_1 and the use of "V_n" allows for the possibility that we may change the ring voltage when n is changed. This axial shift has the same functional form obtained by the earlier treatments.[17–19] However, at this point, we wish only to analyze the effect that this perturbation has on the other two normal modes under the actual experimental conditions in which ω_z is frequency locked. Thus, we now specify that $V_n=V_0+nq_1d^2/a^3$ which produces the results that $\bar{\omega}_{z,n}=\bar{\omega}_{z,0}$ for all n. The radial equation of motion can

now be written in the form

$$\ddot{\rho}-\omega_c\times\dot{\rho}=\left[\frac{q_1V_n}{2m_1d^2}+\Delta_n\right]\rho$$
$$=\left[\frac{\bar{\omega}_{z,n}^2}{2}+\frac{3\Delta_n}{2}\right]\rho\ , \tag{7}$$

where ω_c is given by Eq. (1c). The solution for the resulting compound motion in the xy plane is represented by epicycles with shifted frequencies given by

$$2\omega_\pm=\omega_c\pm(\omega_c^2-2\bar{\omega}_{z,n}^2-6\Delta_n)^{1/2}\ . \tag{8}$$

From this solution, it follows that

$$\omega_-+\omega_+=\omega_c,\quad \omega_+\omega_-=\frac{\bar{\omega}_{z,n}^2}{2}+\frac{3\Delta_n}{2}\ , \tag{9}$$

where we identify ω_+ as the observed (fast) cyclotron frequency $\bar{\omega}_c$, and ω_- as the observed (slow) magnetron rotation frequency, $\bar{\omega}_m$. Thus, these frequencies become

$$\bar{\omega}_{m,n}=\frac{\bar{\omega}_{z,n}^2}{2\bar{\omega}_{c,n}}+\frac{3\Delta_n}{2\bar{\omega}_{c,n}}\ ,$$
$$\bar{\omega}_{c,n}=\omega_c-\bar{\omega}_{m,n}\ . \tag{10}$$

For our experimental conditions, these frequencies become

$$\bar{\omega}_{z,n}=\bar{\omega}_{z,0}=\text{const}\ ,$$
$$\bar{\omega}_{m,n}=\bar{\omega}_{m,0}+\frac{3\Delta_n}{2\bar{\omega}_{c,n}}\ , \tag{11}$$
$$\bar{\omega}_{c,n}=\bar{\omega}_{c,0}-\frac{3\Delta_n}{2\bar{\omega}_{c,n}}\ ,$$

where $\bar{\omega}_{m,0}$ and $\bar{\omega}_{c,0}$ represent the magnetron and cyclotron frequencies, respectively, in the limit that $n\to 0$.

For completeness, we note that the familiar quadrature equation[21]

$$\omega_c^2=\bar{\omega}_c^2+\bar{\omega}_z^2+\bar{\omega}_m^2\ , \tag{12}$$

which has been shown to be invariant under the dominant electrostatic perturbations of trap angle with the magnetic field and trap ellipticity, can be modified to include the perturbations due to image charge if Δ_n is known for the trap. This is done by adding one simple term and is derived algebraically by squaring $\bar{\omega}_{c,n}=\omega_c-\bar{\omega}_{m,n}$ and using Eq. (11). The final result is

$$\omega_c^2=\bar{\omega}_{c,n}^2+\bar{\omega}_{z,n}^2+\bar{\omega}_{m,n}^2+3\Delta_n\ . \tag{13}$$

This is equivalent to extrapolating $\bar{\omega}_{c,n}\to\bar{\omega}_{c,0}$ and $\bar{\omega}_{m,n}\to\bar{\omega}_{m,0}$ prior to using the quadrature Eq. (12) with ω_z frequency locked.

For comparison with the observed number dependency summarized in Table I we rewrite the magnetron (or negative cyclotron) shift as an absolute frequency δ_n given approximately by $\frac{3}{2}\Delta_n/\omega_c$:

$$\delta_n=\left[\frac{3q_1c}{2a^3B_0}\right]n\ . \tag{14}$$

First, we note that this frequency depends linearly on the total trapped charge nq_1 but not mass. It also scales inversely as the cube of the characteristic dimension of the trap. In addition, the relative shift in the observed cyclotron frequency scales as the total trapped mass nm_1, and is independent of charge:

$$\frac{\delta_n}{\omega_c}=\left[\frac{3m_1c^2}{2a^3B_0^2}\right]n\ , \tag{15}$$

which is as observed. Note that the electrostatic well depth does not enter and therefore reductions in V_0 to reduce ω_m (which usually works for electrostatic trap perturbations) will not help. Upon comparing δ_1 [from Eq. (15) for $n=1$] with our experimental shift (average from Table I, fifth column), the radius of the appropriate sphere is 0.156 cm or $\approx R_0$. This is illustrated in Fig. 5 where the sphere is superimposed into the trapping volume.

To see if this model is justified for ions near the trap center, we take a simple average of the $1/a^3$ dependence over solid angle in order to deduce an average spherical radius a^*, which best approximates the real trapping contours:

$$\int_{\text{sphere}}\frac{d\Omega}{(a^*)^3}=\int_{\text{ring}}\frac{d\Omega}{r^3}+\int_{\text{guard}}\frac{d\Omega}{r^3}$$
$$+\int_{\text{endcap}}\frac{d\Omega}{r^3}\ . \tag{16}$$

In this equation, the ring electrode is defined by $\rho^2=R_0^2+2z^2$ whereas the endcap is defined by $\rho^2=2z^2-2Z_0^2$. The integral over the guard electrode is included for completeness, but can be safely ignored because of the $1/r^3$ dependence. Actually, it reduces the final result by $\approx 1.5\%$, but this is compensated for by ignoring the four gaps that exist in the quadring (whose effect is to increase the result by $\approx 1.5\%$). Upon computing the integrals and using the relationship $Z_0=0.72R_0$ for our trap, we find that the effective sphere radius is

$$a^*=1.12R_0\ , \tag{17}$$

which can be compared with our measured number determined from data in Table I ($R_0=0.158$ cm):

$$a=0.99(6)R_0\ . \tag{18}$$

This is quite reasonable agreement considering the simplicity of the average.

Finally, a numerical relaxation program has been used to calculate the fields due to the surface charge induced on the surrounding electrodes by the trapped ion. In particular, this analysis can determine the fractional shift in the axial frequency due to these surface charges. From Eq. (6), this fractional frequency shift is given by

$$\frac{\delta\omega_z}{\omega_z}=-\frac{nq_1d^2}{2a^3V_0} \tag{19}$$

for the spherical model. For the results listed in Table I for protons, this shift becomes $-14(2)$ ppb per trapped

proton. The numerical relaxation program yields a prediction of -15 ppb per proton for this same fractional shift. Thus, this agreement along with the results of the simple average shown in Eq. (16) indicate that we do indeed understand the number dependency of the cyclotron and magnetron resonances and can therefore use the image charge model as a guide to minimize and/ or eliminate this systematic effect.

IV. CONCLUSIONS

The correction shown in Eq. (14) makes it graphically clear that, contrary to previous beliefs, this systematic exists even for a single trapped ion. The difference between extrapolating to zero instead of one ion represents an additional correction of 0.24 ppb for protons, 0.47 ppb for $^2H^+$, 0.73 ppb for $^3H^-$, and 2.8 ppb for $^{12}C^{4+}$ (our usual calibration ion). Since our cyclotron linewidths are typically ~ 0.3 ppb and we always attempt to use small clouds of less than 5 ions, calibrated against a single carbon ion, correcting for this systematic to 10% will eliminate it as a major source of error at the 1-eV level of accuracy.

As a further matter of interest, it should be noted that because the electron's cyclotron frequency is 3 orders of magnitude larger than that of a proton, this systematic will not show up at the current level of precision in the g-2 experiments.[2] Unfortunately, given that the relative systematic for cyclotron frequency measurements is linear in the mass of a single ion, the present effort[8] on $^{14}N^{7+}$ or $^{15}N^{7+}$ will show a 14 to 15 times larger shift than protons in the same trap. In fact, if a single $^{238}U^{92+}$ ion were being investigated,[11] the relative shift would be over 200 times larger. However, from Eq. (15), it is clear that this effect can be greatly reduced by increasing the trap's size. For the $^{238}U^{92+}$ experiment, the relative shift could be made the same as for a single proton in the present trap if we scaled it up by a factor of 6. However, a correction could easily be applied again at the 10% level, suggesting that trap size need only be scaled up by three to achieve relative precision of 2×10^{-10} in a $^{238}U^{92+}$ mass measurement. The loss in coupling to the ion in a larger trap is easily compensated for by the increase in charge state since absolute axial linewidths scale as $q_1^2/m_1 d^2$.

ACKNOWLEDGMENTS

We would like to thank Lowell Brown for helpful discussions and Howard Shugart (University of California, Berkeley) for constructive input during his sabbatical stay at the University of Washington. This work is supported by the National Science Foundation under the "Mono Ion Research" Grant No. PHY87-05397.

[1] R. S. Van Dyck, Jr., D. J. Wineland, P. A. Ekstrom, and H. G. Dehmelt, Appl. Phys. Lett. **28**, 446 (1976); G. Gabrielse, Phys. Rev. A **27**, 2277 (1983).

[2] R. S. Van Dyck, Jr., P. B. Schwinberg, and H. G. Dehmelt, Phys. Rev. D **34**, 722 (1986); Phys. Rev. Lett. **59**, 26 (1987).

[3] P. B. Schwinberg, R. S. Van Dyck, Jr., and H. G. Dehmelt, Phys. Lett. **81A**, 119 (1981).

[4] R. S. Van Dyck, Jr., F. L. Moore, D. L. Farnham, and P. B. Schwinberg, Int. J. Mass Spectrom. Ion Phys. **66**, 327 (1985); Bull. Am. Phys. Soc. **31**, 244 (1986).

[5] F. L. Moore, D. L. Farnham, P. B. Schwinberg, and R. S. Van Dyck, Jr., Bull. Am. Phys. Soc. **34**, 99 (1989). Also R. S. Van Dyck, Jr. F. L. Moore, D. L. Farnham, and P. B. Schwinberg, in *Frequency Standards and Metrology,* edited by A. De Marchi (Springer-Verlag, Berlin, Heidelberg, 1989), p. 349.

[6] G. Gabrielse, in *Fundamental Symmetries,* edited by P. Bloch, P. Pavlopoulos, and R. Klapisch (Plenum, New York, 1987), p. 59.

[7] F. Kern *et al.*, in *Nuclei Far From Stability,* Proceedings of the Fifth International Conference on Nuclei Far From Stability, AIP Conf. Proc. No. 164, edited by Ian S. Towner (AIP, New York, 1987), p. 22.

[8] R. S. Van Dyck, Jr. *et al.*, Phys. Scr. **T22**, 228 (1987).

[9] G. Werth, Metrologia **22**, 174 (1986).

[10] R. M. Weisskoff *et al.*, J. Appl. Phys. **63**, 4599 (1988); R. M. Weisskoff, Ph.D. thesis, Massachussetts Institute of Technology, 1988.

[11] F. L. Moore, D. L. Farnham, P. B. Schwinberg, and R. S. Van Dyck, Jr., Phys. Scr. **T22**, 294 (1988).

[12] F. L. Moore, D. L. Farnham, P. B. Schwinberg, and R. S. Van Dyck, Jr., in the Proceedings of the 1989 Lawrence Berkeley Workshop on Highly Charged Ions [Nucl. Instrum. Methods (to be published)].

[13] R. S. Van Dyck, Jr., P. B. Schwinberg, and S. H. Bailey, in *Atomic Masses and Fundamental Constants 6,* edited by J. A. Nolen, Jr. and W. Benenson (Plenum, New York, 1980), p. 173.

[14] R. S. Van Dyck, Jr., P. B. Schwinberg, and H. G. Dehmelt, in *New Frontiers in High Energy Physics* (Plenum, New York, 1978), p. 159.

[15] L. Brown and G. Gabrielse, Rev. Mod. Phys. **58**, 233 (1986).

[16] R. S. Van Dyck, Jr. and P. B. Schwinberg, Phys. Rev. Lett. **47**, 395 (1981).

[17] D. Wineland and H. Dehmelt, J. Appl. Phys. **46**, 919 (1975).

[18] L. S. Brown, K. Helmerson, and J. Tan, Phys. Rev. A **34**, 2638 (1986).

[19] H. Dehmelt, in *Laser Spectroscopy VIII,* edited by W. Persson and S. Svanberg (Springer-Verlag, Berlin, 1987), p. 39.

[20] J. D. Jackson, in *Classical Electrodynamics* (Wiley, New York, 1962), p. 28.

[21] L. Brown and G. Gabrielse, Phys. Rev. A **25**, 2423 (1982).